Analysis of Face Slabs in Concrete-Faced Rockfill Dams under Earthquake Ground Motions

Miad Saberi[1], Charles-Darwin Annan[2], Jean-Marie Konrad[3]

[1] Ph.D, Geomechanical Engineering Analysis, GHD – Montréal, QC, Canada.
[2] Associate Professor, Department of Civil and Water Engineering, Université Laval – Québec, QC, Canada.
[3] Professor, Department of Civil and Water Engineering, Université Laval – Québec, QC, Canada.

ABSTRACT

Over the past few decades, many Concrete-Faced Rockfill Dams (CFRD) have been constructed around the world. The structural complexity of this dam type and the high social, environmental and economic costs associated with failure require reliable analysis techniques to understand its behaviour and performance. Current design practices are largely empirical for lack of sufficient observational evidence, particularly under earthquake dynamic loading. Earthquake ground motion is an important phenomenon that has caused serious damage to the impervious concrete face slab laid on the upstream of CFRDs, and any failure and damage in the face slab may result in dam instability. The behaviour of the concrete face slab is mainly governed by the interaction between the concrete slab and the cushion layer. In this study, the seismic behaviour of the concrete face slab in CFRDs is investigated using an advanced interface constitutive model to simulate the face slab-cushion layer interaction. The interface model is capable of simulating complex stress-displacement and volumetric behaviour of granular soil-structure interfaces. The effect of the reservoir water level on the seismic response of the concrete face slab is also investigated. The results illustrate that the earthquake ground motion can significantly increase the face slab response when compared with the static condition, and that the water level plays an important role in the face slab behaviour under strong ground motion.

Keywords: concrete faced rockfill dam, interface, concrete face slab, earthquake ground motion, reservoir water level.

INTRODUCTION

Concrete faced rockfill dams (CFRD) have been constructed increasingly over the past three decades. This is due to its low-cost and simple and rapid construction process [1–3]. CFRDs generally consist of five important parts, including four zones (i.e. cushion, transition, main rockfill and secondary rockfill zones) and a concrete face laid on the upstream of the dam as illustrated in Figure . *1*. In CFRDs, the structural integrity of the concrete face slab is of critical consideration for designers and dam owners. Failure or damage to this impervious section of the dam would result in water penetration into the rockfill body and consequently weaken the dam stability [4–7]. Earthquake ground motion is an important phenomenon that has caused severe damage to concrete face slabs in CFR dams [8,9].

One of the critical behavior parameters in CFRDs is the behavior of the interface region between the concrete face slab and the cushion layer made of gravel or rockfill. The interface plays an important role because of the interaction between the two main dam bodies with very different stiffnesses. The concrete slab-cushion layer interaction has been simulated widely by the contact analysis with Coulomb's friction law (e.g. [2,4,10–13]) and by zero-thickness elements with no volume change (e.g. [8,9,14,15]). Experimental observations (e.g. [16–19]), however, indicate that the granular soil-structure interface has a thickness of about (5-10) D_{50} of adjacent granular soil and therefore exhibits behavior different from its adjacent materials. The interface zone shows complicated volumetric behavior (i.e. phase transformation from contraction to dilation under shearing, accumulative contraction under cyclic loading and particle breakage) and stress-displacement relationships (i.e. stress hardening/softening, stress degradation, and stress path dependency) under different loading conditions. The interface may experience particle breakage under shear cycles, even at low to medium normal stresses [17,20,21]. This phenomenon significantly increases the accumulative contraction behavior at the interface zones.

The essential behaviors of granular soil-structure interfaces outlined above (i.e. phase transformation, accumulative contraction, particle breakage effect, critical state, stress hardening and degradation) cannot be addressed using contact analysis or zero-thickness element with no volume change. The thin-layer interface element proposed by Zienkiewicz et al. [22] and Desai et al. [23] would be a preferred choice due to its capabilities to simulate volumetric behavior. This element type, however, needs
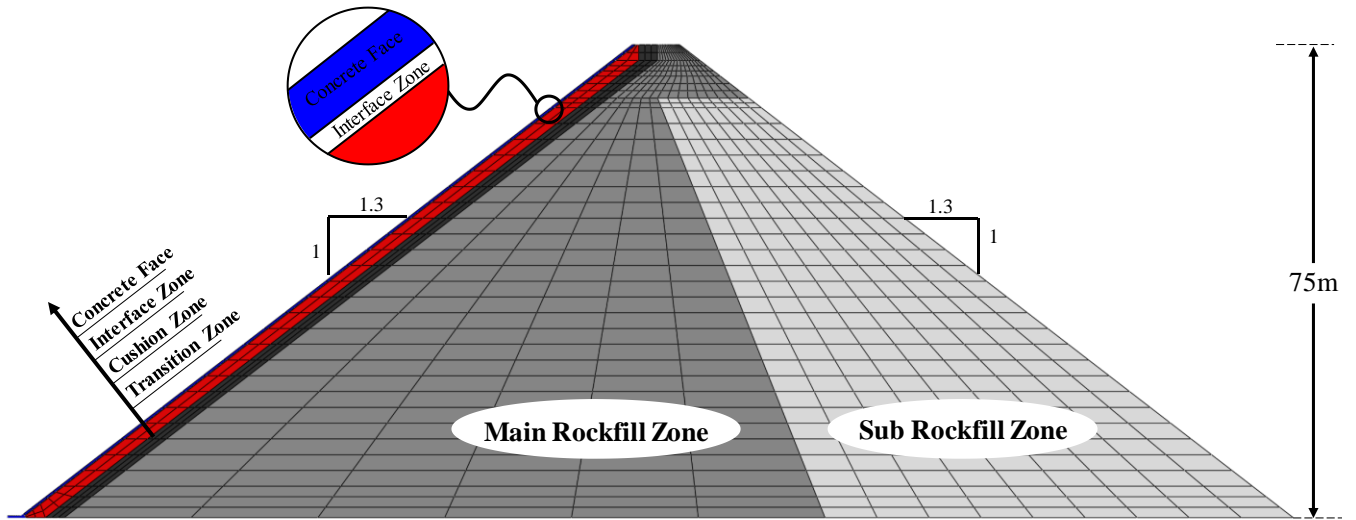
Figure . 1 Typical cross section of the selected CFR dam

to be used with an advanced interface constitutive model if it is to address the complex behaviors of granular soil-structure interface systems identified above.

This paper presents the seismic response of CFRDs by considering the effect of concrete slab-cushion layer interaction using an advanced interface constitutive model recently developed by the authors [24,25]. The model is in the framework of two-surface plasticity and critical state soil mechanics, and is capable of simulating the complex behavior of granular soil-structure interfaces under monotonic and cyclic loading, such as phase transformation, critical state, accumulative contraction, stress hardening, stress degradation, stress path dependency and particle breakage under shear cycles. The constitutive model is implemented into a finite element code as a thin-layer interface element, and used in the response analysis of a typical concrete faced rockfill dam under earthquake ground motions. The performance of the concrete face slab are compared under static and seismic conditions and the effect of reservoir water levels on the stress and deflection response of concrete face slab is investigated.

NUMERICAL MODEL

Geometry and Material

A typical CFR dam with 75 m high built on a bedrock foundation is selected for the analysis of this study. The thickness of the concrete slab on the upstream face of the selected dam is 0.3 m. The dam has a crest width of about 7 m and the side slopes of 1.3 H : 1V down to the foundation level. The general view and cross section of the dam are shown in Figure . 1. In this study, a general purpose finite element (FE) software ABAQUS [26] was used as a numerical tool for simulating the CFR dam.

The Drucker–Prager constitutive model [27] has been used widely for simulating granular materials, such as rockfill, in dam analysis (e.g. [7,13,28]).The modified Drucker–Prager or Cap plasticity model originally proposed by DiMaggio and Sandler [29] and Sandler and Baron [30] has also been widely used (e.g. [31,32]). In the present study, the cap plasticity model is used to simulate the rockfill zones of the selecetd dam. The cap plasticity model employed considers the effect of stress history, stress path, dilatancy, and intermediate principal stress. The yield surface of the model has three segments: Drucker–Prager shear failure surface (F_s), an elliptical cap (F_c) surface and a transition surface (F_t) between the shear failure surface and the cap. The cap plasticity model simulates the elastic behavior using a linear elastic formulation once when the stress state is within the yield surface. The elasto-plastic behavior is simulated once the stress state is on the yield surface. The formulation of Drucker–Prager failure surface, cap yield surface and transition surface are presented in Eqs. (1), (2) and (3) respectively.

$$F_s = t - ptan\beta - d = 0 \tag{1}$$

$$F_c = \sqrt{(p - p_a)^2 + \left(\frac{Rt}{1 + \alpha - \alpha/cos\beta}\right)^2} - R(d + p_a tan\beta) = 0 \tag{2}$$

Table 1 Cap plasticity model parameters for rockfill materials

Parameters	Zone			
	Cushion	**Transition**	**Main Rockfill**	**Sub Rockfill**
Mass Density, ρ (Kg/m³)	2000	2000	1980	1980
Young's modulus, E (MPa)	200	200	100	110
Poisson's ratio, υ	0.2	0.2	0.2	0.2
Cohesion, d (MPa)	1×10^{-5}	1×10^{-5}	1×10^{-5}	1×10^{-5}
Friction angle, β (deg)	57	56.5	62	61
Transition surface radius, α	0.01	0.01	0.01	0.01
Flow stress ratio, K	1.0	1.0	1.0	1.0
Cap eccentricity, R	0.4	0.45	0.1	0.1

$$F_t = \sqrt{(p - p_a)^2 + \left[t - \left(1 - \frac{\alpha}{cos\beta}\right)(d + p_a tan\beta)\right]^2} - \alpha(d + p_a tan\beta) = 0 \tag{3}$$

Where p is mean effective stress, d and β are cohesion and soil friction angle in the p-t. In Eq. 1, t is a measure of deviatoric stress and is calculated as $t=q/g$, in which q is deviatoric stress and g is a function controlling the shape of yield surface in the deviatoric plane (Π-Plane) defined by Eq. (4).

$$g = \frac{2K}{1 + K + (1 - K)\left(r/q\right)^3} \tag{4}$$

where K is a model parameter and r is the third invariant of deviatoric stress.

In Eq. 2, R is a model parameter, α is a small number defined for a smooth transition surface between the Drucker–Prager and the cap failure surfaces, and p_a is an evolution term. The model totally requires eight parameters to simulate elasto-plastic behavior of granular soils. The details about the model formulation and parameter identification can be found in Helwany [32]. As can be observed in FigureFigure . 1, the CFR dam in the present study consists of four rockfill zones (cushion zone, transition zone, main rockfill zone and sub rockfill zone). The model parameters for these four zones were estimated using triaxial test data obtained by Marachi et al. [33] and Marsal [34] for large rockfill materials. The rockfill material parameters used in this study are provided in Table 1.

The interface between the concrete slab and the cushion layer is simulated using an interface thin-layer element with the advanced constitutive model proposed by the authors [24,25]. The model is based on a two dimensional (2D) plane strain problem. The thickness (t) of the interface zone is assumed to be 5-10 times the mean effective diameter (D_{50}) of adjacent soil particles. Stress and strain vectors in the interface model consist of normal and tangential components. The detailed description of the formulation of the interface constitutive model for the soil-structure interfaces can be found in [24,25]. For the sake of completeness, however, a brief summary is presented in Table 2.

Based on previous study [17,20,21,35], granular soil-structure interfaces may experience particle breakage during shear cycles which results in more accumulative contraction. Laboratory tests also show that particle breakage translates the critical state line (CSL) downward towards smaller void ratio in the *e-logp´* plane [36]. In the interface model, for simulating the effect of particle breakage, the CSL is translated towards smaller void ratio in the e-$ln(\sigma_n/p_{atm})$ plane by reformulating the approach suggested by Liu and Zou [37] for monotonic behavior of gravelly soils (Eq. (8-10).

The interface model used for simulating the interface zone between the concrete face and cushion layer requires ten calibration parameters in total: two for elasticity (D_{t0} and D_{n0}), three for critical state (e_{cs-0}, λ and μ^{cs}), two for dilatancy (A^d and K^d) and one for hardening (K_{p0}) and two for particle breakage (b_{r1} and b_{r2}). The details regarding the model parameters determination can be found in Saberi et al. [24,25].

Table 2 Constitutive equations of the interface model and model parameters

Constitutive formulation	Eq.	Discription	Parameters
Elasticity			
$\dot{\boldsymbol{\sigma}} = \boldsymbol{D}^e \dot{\boldsymbol{\varepsilon}}^e =$ $= \begin{bmatrix} D_{n0}\sqrt{\sigma_n/p_{atm}} & 0 \\ 0 & D_{t0}\sqrt{\sigma_n/p_{atm}} \end{bmatrix} \dot{\boldsymbol{\varepsilon}}^e$	(5)	$\boldsymbol{D}^e$: elastic stiffness matrix [38–40] D_n: elastic normal stiffness D_t: elastic tangential stiffness p_{atm}: atmospheric pressure, given by 101(kPa)	D_{n0} and D_{t0}
Model Surfaces			
Yield surface			
$f = \dfrac{\tau}{\sigma_n} - \alpha - sm = 0$	(6)	*f:* yield surface function[39–41] τ/σ_n: stress ratio (μ), α: back stress ratio and the slope of yield surface bisector (i.e. $\alpha=\mu-m$) m: controls the size of the yield surface, given by $0.01\mu^{cs}$-$0.05\mu^{cs}$ [42] s: auxiliary parameter [41]	
$s = \begin{cases} +1 & \mu - \alpha \geq 0 \\ -1 & \mu - \alpha < 0 \end{cases}$	(7)		
Critical state surface			
$\psi = e - \left(e_{cs-0}(1 - B_r) - \lambda\ln(\sigma_n/p_{atm})\right)$	(8)	ψ: state parameter [39,43,44] e: void ratio at the current state e_{cs}: critical state void ratio corresponding to the current value of σ_n. B_r: degree of particle breakage [45] w_p: modified plastic work [46] $<\,>$: Macaulay brackets; $<x>= x$ if x>0, and $<x>= 0$ if x≤0. τ^{cs}: shear stress at critical state σ_n^{cs}: normal stress at critical state μ^{cs}: slope of the critical state surface in σ_n-τ plane (i.e. critical state stress ratio)	e_{cs-0}, λ, b_{r1}, b_{r2} and μ^{cs}
$B_r = \dfrac{w_p}{b_{r1} + b_{r2}w_p}$	(9)		
$W_p = \int \left(\sigma_n\langle\dot{\varepsilon}_n^p\rangle + \tau\dot{\varepsilon}_t^p\right)$	(10)		
$\tau^{cs}/\sigma_n^{cs} = \mu^{cs}$	(11)		
Dilatancy surface			
$\mu^d = \mu^{cs} \exp\left(K^d\psi\right)$	(12)	μ^d: dilatancy stress ratio D: dilatancy coefficient [41] Γ: loading index [47] $\boldsymbol{R}$: direction of increment of plastic strain vector [39,41] $\boldsymbol{n}$: vector normal to yield surface f K_p; plastic modulus	K^d, A^d and K_{p0}
$D = \dfrac{\dot{\varepsilon}_n^p}{|\dot{\varepsilon}_t^p|} = A^d(d^d) = A^d(\mu^d - s\mu)$	(13)		
$\dot{\boldsymbol{\varepsilon}}^p = \begin{Bmatrix} \dot{\varepsilon}_n^p \\ \dot{\varepsilon}_t^p \end{Bmatrix} = \langle\Gamma\rangle\boldsymbol{R}$	(14)		
$\Gamma = \boldsymbol{n}^T\dot{\boldsymbol{\sigma}}/K_p$	(15)		
$\boldsymbol{R} = \begin{Bmatrix} R_n \\ R_t \end{Bmatrix} = \begin{Bmatrix} D \\ \partial f/\partial\tau \end{Bmatrix}$	(16)		
$\boldsymbol{n} = \begin{Bmatrix} \partial f/\partial\sigma_n \\ \partial f/\partial\tau \end{Bmatrix}$	(17)		
$K_p = K_{p0}D_{t0}\sqrt{\sigma_n/p_{atm}}\dfrac{(\mu^f - s\alpha)}{|\alpha|}$	(18)		

A typical interface behavior between a concrete slab and gravelly cushion layer in CFRDs was experimentally studied by Zhang and Zhang [48]. In the present study, the parameters of the interface model was calibrated using those laboratory test data. The average grain size of the gravelly soils at the in interface zone was 20 mm with dry unit weight of 21.5 kN/m^3. The interface thickness was also 100 mm. The values of the interface model parameters are presented in Table 3.

Table 3 Interface Model parameters for the CFR dam

Elasticity		Critical state			Dilatancy		Hardening	Particle breakage	
D_{t0} (MPa)	D_{n0} (MPa)	e_{cs-0}	λ	μ^{cs}	A^d	K^d	K_{p0}	b_{r1}(MPa)	b_{r2}
5.0	6.0	0.27	0.01	0.88	0.4	6.0	0.68	6.5	1

The concrete face slab in this study is simulated by a linear elastic model. It is assumed to have a mass density ρ= 2400 kg/m³, elasticity Young's modulus E=25 GPa, and Poisson's ratio υ= 0.17.

Loading

In the current study, the construction and impoundment processes were simulated using 40 sub-steps (i.e. 25 stages for dam construction and 15 stages for impoundment), and the water levels were simulated by the hydrostatic pressures on the concrete face. A earthquake record with magnitude 5 previously recorded in Rivière-du-Loup, Quebec, Canada were selected for the analyses. This ground motion was recorded in station NHN with PGA=0.53g. The acceleration time history of the earthquake record is illustrated in Figure . 2. In the finite element analysis of this study, the earthquake excitations is applied at the bottom of the dam.

NUMERICAL RESULTS

In this section, the performance of the concrete face slab of CFRDs under static and seismic loading condition is investigated. The distributions of maximum slope direction (i.e. parallel with face slab) compressive stress, maximum horizontal compressive stress of concrete face slab and maximum slab deflection on the height of the dam are examined. For these analyses, the reservoir water level is assumed to be full. The effect of reservoir water level on the seismic response of face slab is also explored in this study. As can be observed from Figure . 3, the response of the concrete face slab significantly increases under earthquake ground motion compared with the static condition. The maximum compressive stresses in the slope direction and horizontal direction of the face slab experience about 60% and 65% increase under seismic condition respectively (Figure . 3-a and Figure . 3-b). The maximum slab deflection also increases from about 0.27 m (i.e. 0.36 H%, where H is dam height) in the static condition to about 0.34 m (i.e. 0.45H%) under the earthquake condition (Figure . 3-c).

Regarding the effect of water level on seismic response of concrete face slab, different reservoir water levels (i.e. 40m, 60m, and full reservoir) are modeled and subjected to the selected earthquake excitation. Results of the numerical predictions for face slab stresses and deflection are presented in Figure . 4. The maximum compressive stresses in the both slope and horizontal directions experience considerable increases as can be observed in Figure . 4-a and Figure . 4-b. The maximum stress in the slope direction of the face slab increases by 47% as the reservoir water level rises from 40 m to its full condition under the earthquake loading condition. It is also evident from Figure . 4 that the location of maximum stresses move up the face slab with increasing reservoir water level. The maximum distribution of face slab deflection under earthquake ground motion also increases significantly by increasing reservoir water level as can be observed in Figure . 4-c. The maximum deflection increases from 0.14 m for reservoir water level of 40 m to about 0.34 m for the full reservoir condition.
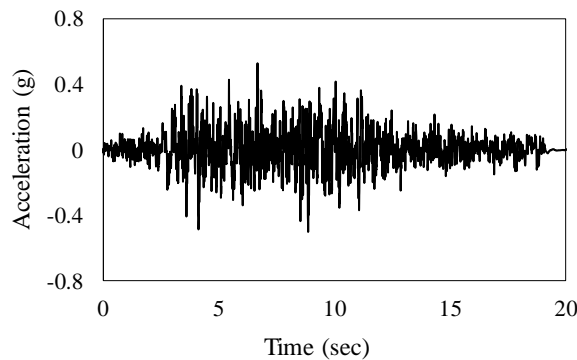

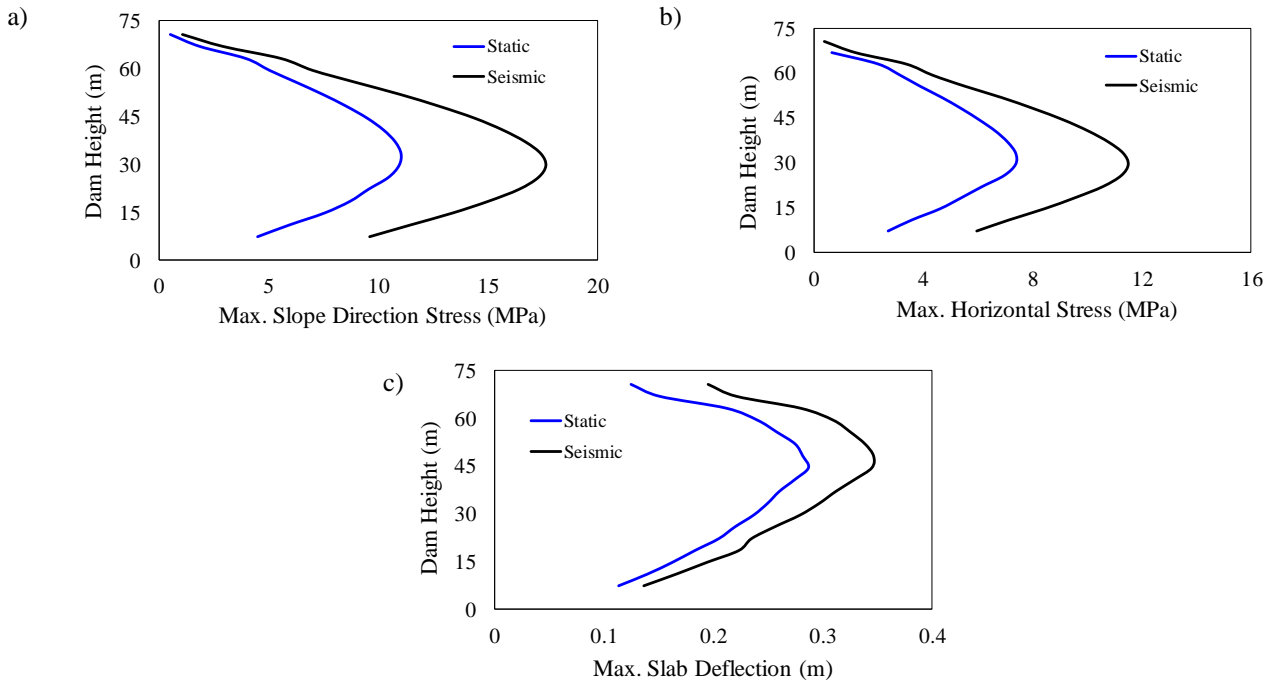
Figure . 2 Input ground motion time history

a)

b)

c)

Figure . 3 Static and seismic responses of concrete face slab, a) slope direction stress, b) horizontal stress, c) slab deflection.

CONCLUSION

This paper has presented a numerical study on the behavior of the concrete face slab in CFRDs by considering the concrete slab-cushion layer interaction under earthquake excitation. The interface zone was simulated using the thin-layer interface elements defined by an advance constitutive model capable of simulating complex behavior of granular soil-structure interfaces
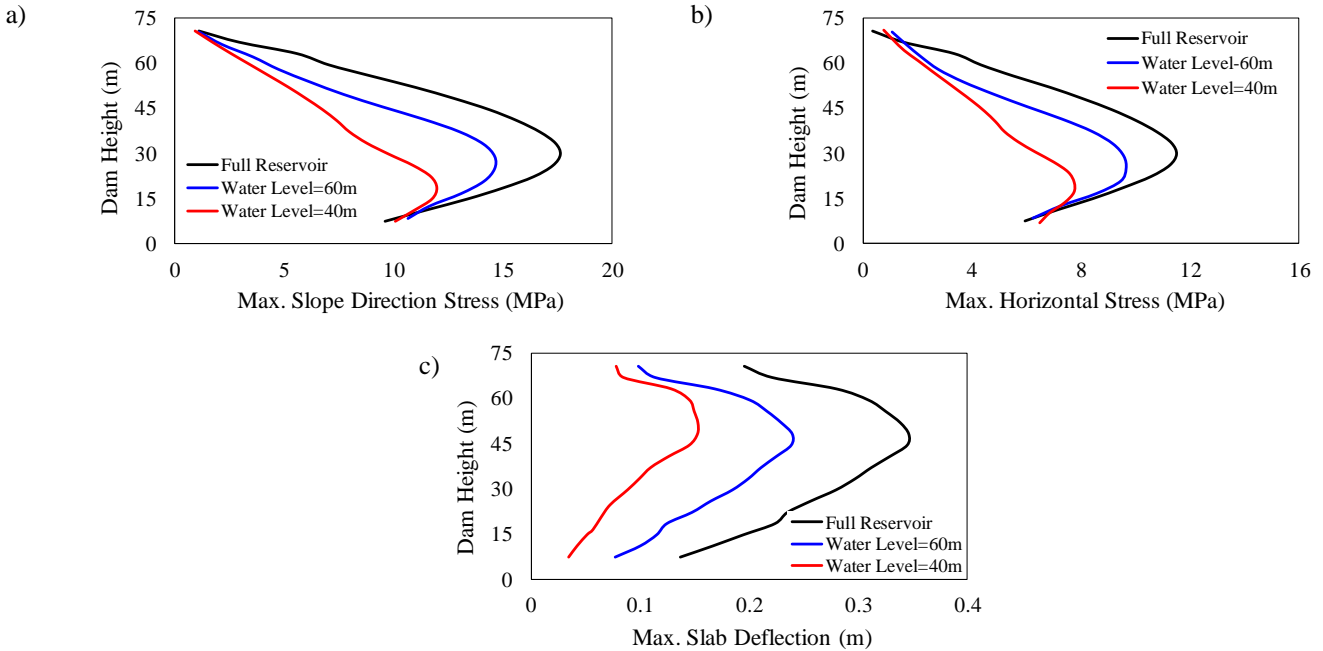
a)

b)

c)

Figure . 4 Reservoir water level effect on the seismic responses of concrete face slab, a) slope direction stress, b) horizontal stress, c) slab deflection.

such (stress hardening, critical state, stress degradation, accumulative contraction and particle breakage). The performance of concrete face slab under static and seismic loading conditions was investigated, and the effect of reservoir water level on the stress response and deflection of the concrete face slab were studied.

Earthquake ground motion significantly increase the responses of the concrete face slab, such as slope-direction and horizontal stresses, and face slab deflection compared with the static condition. The face slab stresses (i.e. slope direction and horizontal) and deflection also experience considerable increases by an increase in reservoir water level.

ACKNOWLEDGMENTS

REFERENCES

[1]   Sherard JL, Barry Cooke J. CONCRETE-FACE ROCKFILL DAM: I. ASSESSMENT. J Geotech Eng 1987;113:1096–112.

[2]   Uddin N, Gazetas G. Dynamic Response of Concrete-Faced Rockfill Dams to Strong Seismic Excitation. J Geotech Eng 1995;121:185–97. doi:doi:10.1061/(ASCE)0733-9410(1995)121:2(185).

[3]   Gazetas G, Dakoulas P. Seismic analysis and design of rockfill dams: state-of-the-art. Soil Dyn Earthq Eng 1992;11:27–61.

[4]   Dakoulas P. Longitudinal vibrations of tall concrete faced rockfill dams in narrow canyons. Soil Dyn Earthq Eng 2012;41:44–58. doi:10.1016/j.soildyn.2012.05.010.

[5]   Uddin N. A dynamic analysis procedure for concrete-faced rockill dams subjected to strong seismic excitation. Comput Struct 1999;72:409–21. doi:10.1016/S0045-7949(99)00011-5.

[6]   Zhou M, Bingyin Z, Chong P, Wu W. Three-dimensional numerical analysis of concrete-faced rockfill dam using dual-mortar finite element method with mixed tangential contact constraints. Int J Numer Anal Methods Geomech 2016;40:2100–22. doi:10.1002/nag.

[7]   Saberi M, Annan C-D, Konrad J-M. Numerical analysis of concrete-faced rockfill dams considering effect of face slab – cushion layer interaction. Can Geotech J 2018;55:1489–501. doi:10.1139/cgj-2017-0609.

[8]   Zou D, Xu B, Kong X, Liu H, Zhou Y. Numerical simulation of the seismic response of the Zipingpu concrete face rockfill dam during the Wenchuan earthquake based on a generalized plasticity model. Comput Geotech 2013;49:111–22. doi:10.1016/j.compgeo.2012.10.010.

[9]   Xianjing K, Yang Z, Degao Z, Bin X, Long Y. Numerical analysis of dislocations of the face slabs of the Zipingpu Concrete Faced Rockfill Dam during the Wenchuan earthquake. Earthq Eng Eng Vib 2011;10:581–9. doi:10.1007/s11803-011-0091-z.

[10]   Seiphoori A, Haeri SM, Karimi M. Three-dimensional nonlinear seismic analysis of concrete faced rockfill dams subjected to scattered P, SV, and SH waves considering the dam–foundation interaction effects. Soil Dyn Earthq Eng 2011;31:792–804.

[11]   Wen L, Chai J, Xu Z, Qin Y, Li Y. Monitoring and numerical analysis of behaviour of Miaojiaba concrete-face rockfill dam built on river gravel foundation in China. Comput Geotech 2017;85:230–48. doi:10.1016/j.compgeo.2016.12.018.

[12]   Zhou MZ, Zhang B yin, Jie Y xin. Numerical simulation of soft longitudinal joints in concrete-faced rockfill dam. Soils Found 2016;56:379–90. doi:10.1016/j.sandf.2016.04.005.

[13]   Kartal ME, Bayraktar A, Basaga HB. Nonlinear finite element reliability analysis of Concrete-Faced Rockfill (CFR) dams under static effects. Appl Math Model 2012;36:5229–48. doi:10.1016/j.apm.2011.12.004.

[14]   Bayraktar A, Kartal ME, Adanur S. The effect of concrete slabrockfill interface behavior on the earthquake performance of a CFR dam. Int J Non Linear Mech 2011;46:35–46. doi:10.1016/j.ijnonlinmec.2010.07.001.

[15]   Xu B, Zou D, Kong X, Hu Z, Zhou Y. Dynamic damage evaluation on the slabs of the concrete faced rockfill dam with the plastic-damage model. Comput Geotech 2015;65:258–65. doi:10.1016/j.compgeo.2015.01.003.

[16]   Fakharian K. Three-dimensional monotonic and cyclic behaviour of sand-steel interfaces: Testing and modelling. Ph.D. thesis, University fo Ottawa, Ontario, Canada, 1996.

[17]   Zhang G, Zhang J-M. Monotonic and Cyclic Tests of Interface between Structure and Gravelly Soil. Soils Found 2006;46:505–18.

[18]   DeJong JT, Westgate ZJ. Role of Initial State, Material Properties, and Confinement Condition on Local and Global Soil-Structure Interface Behavior. J Geotech Geoenvironmental Eng 2009;135:1646–60. doi:10.1061/(ASCE)1090-0241(2009)135:11(1646).

[19]   Dejong JT, White DJ, Randolph MF. Microscale observation and modeling of soil-structure interface behavior using particle image velocimetry. Soils Found 2006;46:15–28. doi:10.3208/sandf.46.15.

[20]   Zhang G, Zhang J-M. Constitutive rules of cyclic behavior of interface between structure and gravelly soil. Mech Mater

2009;41:48–59. doi:10.1016/j.mechmat.2008.08.003.

[21]   Saberi M, Annan C-D, Konrad J-M. On the mechanics and modeling of interfaces between granular soils and structural materials. Arch Civ Mech Eng 2018;18:1562–79. doi:https://doi.org/10.1016/j.acme.2018.06.003.

[22]   Zienkiewicz OC, Best B, Dullage C, Stagg KG. Analysis of Nonlinear Problems in Rock Mechanics with Particular Reference to Jointed Rock Systems. 2nd Int. Soc. Rock Mech. Proc., Belgrad: 1970, p. 501–9.

[23]   Desai CS, Lightner JG, Siriwardane h J. Thin-Layer Element for Interfaces and Joints. Int J Numer Anal Methods Geomech 1984;8:19–43.

[24]   Saberi M, Annan C-D, Konrad J-M. Constitutive Modeling of Gravelly Soil-Structure Interface Considering Particle Breakage. J Eng Mech 2017;143:04017044 (14 pp.). doi:10.1061/(ASCE)EM.1943-7889.0001246.

[25]   Saberi M, Annan CD, Konrad JM. Implementation of a soil-structure interface constitutive model for application in geo-structures. Soil Dyn Earthq Eng 2019;116:714–31. doi:10.1016/j.soildyn.2018.11.001.

[26]   Dassault Systèmes. Abaqus Documentation. 2013.

[27]   Drucker DC, Gibson RE, Henkel DJ. Soil Mechanics and Work-Hardening Theories of Plasticity. Trans Am Soc Civ Eng 1957;122:338–46.

[28]   Bayraktar A, Kartal ME. Linear and nonlinear response of concrete slab on CFR dam during earthquake. Soil Dyn Earthq Eng 2010;30:990–1003. doi:10.1016/j.soildyn.2010.04.010.

[29]   DiMaggio FL, Sandler IS. Material Model for Granular Soils. J Eng Mech Div 1971;97:935–50.

[30]   Sandler IS, Baron M. Recent developments in the constitutive modeling of geological materials. Numer. Methods Geomech., Rotterdom: 1979, p. 363–76.

[31]   Loupasakis CJ, Christaras BG, Dimopoulos GC, Hatzigogos TN. Evaluation of Plasticity Models' Ability to Analyze Typical Earth Dams' Soil Materials. Geotech Geol Eng 2009;27:71–80. doi:10.1007/s10706-008-9212-5.

[32]   Helwany S. Applied soil mechanics : with ABAQUS applications. John Wiley & Sons; 2007.

[33]   Marachi ND, Chan CK, Seed H bolton. Evaluation of Properties of Rockfill Materials. J Soil Mech Found Div 1972;98:95–114.

[34]   Marsal RJ. Large-Scale Testing of Rockfill Materials. J Soil Mech Found Div 1967;93:27–43.

[35]   Uesugi M, Kishida H, Tsubakihara Y. Friction between sand and steel under repeated loading. Soils Found 1989;29:127–37. doi:10.3208/sandf.47.887.

[36]   Ghafghazi M, Shuttle DA, Dejong JT. "Closure to Particle breakage and the critical state of sand" by Ghafghazi, M., Shuttle, D.A., and DeJong, J.T. [Soils and Foundations 54 (3) (2014) 451–461]. Soils Found 2015;55:223–5. doi:10.1016/j.sandf.2014.12.019.

[37]   Liu H, Zou D. Associated Generalized Plasticity Framework for Modeling Gravelly Soils Considering Particle Breakage. J Eng Mech 2013;139:606–15. doi:10.1061/(ASCE)EM.1943-7889.0000513. ©.

[38]   Lashkari A. Prediction of the shaft resistance of nondisplacement piles in sand. Int J Numer Anal Methods Geomech 2013;37:904–31. doi:10.1002/nag.

[39]   Saberi M, Annan C-D, Konrad J-M, Lashkari A. A critical state two-surface plasticity model for gravelly soil-structure interfaces under monotonic and cyclic loading. Comput Geotech 2016;80:71–82. doi:10.1016/j.compgeo.2016.06.011.

[40]   Saberi M, Annan C-D, Konrad J-M. A Unified Constitutive Model for Simulating Stress-Path Dependency of Sandy and Gravelly Soil-Structure interfaces. Int J Non Linear Mech 2018.

[41]   Lashkari A. A plasticity model for sand-structure interfaces. J Cent South Univ 2012;19:1098–108. doi:10.1007/s11771-012-1115-1.

[42]   Papadimitriou AG, Bouckovalas GD. Plasticity model for sand under small and large cyclic strains: a multiaxial formulation. Soil Dyn Earthq Eng 2002;22:191–204. doi:10.1016/S0267-7261(02)00009-X.

[43]   Been K, Jefferies MG. A state parameter for sands. Géotechnique 1985;35:99–112. doi:10.1680/geot.1985.35.2.99.

[44]   Liu H, Song E, Ling HI. Constitutive modeling of soil-structure interface through the concept of critical state soil mechanics. Mech Res Commun 2006;33:515–31. doi:10.1016/j.mechrescom.2006.01.002.

[45]   Lade P V., Yamamuro J a., Bopp P a. Significance of Particle Crushing in Granular Materials. J Geotech Geoenvironmental Eng 1996;122:309–16. doi:10.1061/(ASCE)1090-0241(1997)123:9(889).

[46]   Hu W, Yin Z, Dano C, Hicher P-Y. A constitutive model for granular materials considering grain breakage. Sci China Technol Sci 2011;54:2188–96. doi:10.1007/s11431-011-4491-0.

[47]   Dafalias YF. Bounding Surface Plasticity. I: Mathematical Foundation and Hypoplasticity. J Eng Mech 1986;112:966–87.

[48]   Zhang G, Zhang J-M. Unified Modeling of Monotonic and Cyclic Behavior of Interface Between Structure and Gravelly Soil. Soils Found 2008;48:231–45. doi:10.3208/sandf.48.231.